ORIGINAL ARTICLE

Functional roles of graft-infiltrating lymphocytes during early-phase post-transplantation in mouse cardiac transplantation models

Yoshikazu Ganchiku, Ryoichi Goto*, Ryo Kanazawa, Takuji Ota, Kazuaki Shibuya, Yasutomo Fukasaku, Nozomi Kobayashi, Rumi Igarashi, Norio Kawamura, Masaaki Zaitsu, Masaaki Watanabe & Akinobu Taketomi*

Department of Gastroenterological Surgery I, Graduate School of Medicine, Hokkaido University, Sapporo, Hokkaido, Japan

Correspondence
Ryoichi Goto MD, PhD, Kita-14 Nishi-7, Sapporo, Hokkaido, 060-8648, Japan.
Tel.: +81-11-706-5927;
fax: +81-11-717-7515;
e-mail: r-gotoh@mba.ocn.ne.jp
Akinobu Taketomi FACS, MD, PhD, Kita-14 Nishi-7, Sapporo, Hokkaido, 060-8648, Japan.
Tel.: +81-11-706-5927;
fax: +81-11-717-7515;
email: taketomi@med.hokudai.ac.jp

*Both the authors contributed equally as senior authors.

SUMMARY

Immunological behavior of graft-infiltrating lymphocytes (GILs) determines the graft fate (i.e., rejection or acceptance). Nevertheless, the functional alloreactivity and the phenotype of GILs at various times during the early post-transplantation phase have not been fully elucidated. We examined the immunological activities of early-phase GILs using a murine model of cardiac transplantation. GILs from 120-h allografts, but not 72-h allografts, showed robust activation and produced proinflammatory cytokines. In particular, a significant increase in $CD69^+T\text{-}bet^+Nur77^+$ T cells was detected in 120-h allografts. Furthermore, isolated GILs were used to reconstitute BALB/c $Rag2^{-/-}\gamma c^{-/-}$ (BRG) mice. BRG mice reconstituted with 120-h GILs displayed donor-specific immune reactivity and rejected donor strain cardiac allografts; conversely, 72-h GILs exhibited weak anti-donor reactivity and did not reject allografts. These findings were confirmed by re-transplantation of cardiac allografts into BRG mice at 72-h post-transplantation. Re-transplanted allografts continued to function for >100 days, despite the presence of $CD3^+$ GILs. In conclusion, the immunological behavior of GILs considerably differs over time during the early post-transplantation phase. A better understanding of the functional role of early-phase GILs may clarify the fate determination process in the graft-site microenvironment.

Introduction

The cytotoxic ability of graft-infiltrating lymphocytes (GILs) determines the immune balance and eventual fate of allografts [1,2]. During the early phase of organ transplantation, alloantigen-specific naïve lymphocytes are activated via antigen presentation in secondary lymphoid tissues [3], and an interval of 4–5 days is required to acquire sufficient immune activity [4]. Subsequently, the activated lymphocytes infiltrate into transplanted organs and exert cytotoxic effects. However, recipient-derived lymphocytes infiltrate vascularized grafts within

24 h [4,5]. The immunological behavior of these early-phase GILs remains unclear. Previous reports showed that these subsets with memory phenotype demonstrated an alloantigen-specific proinflammatory ability; they were activated by an alloantigen-dependent mechanism, secreted proinflammatory cytokines, and promoted allograft rejection [4–10]. In infectious diseases, such lymphocytes with a memory phenotype which infiltrate inflammatory sites during very early phase of infection are presumed to have antigen-nonspecific protective functions; they induced antigen-nonspecific inflammatory reactions independent of their repertoire, maintained inflammatory responses to non-self-antigens, secreted proinflammatory cytokines and promoted the trafficking of primed antigen-specific effector T cells [4,6,7,11–15]. Although accumulating evidences indicate that early-phase GILs have allogeneic function, however, the removal of early-phase GILs failed to induce transplant tolerance [16–18]. These findings indicate that early-phase GILs exhibit the heterogeneous immunological behavior. Moreover, the other findings that, in both transplant and nontransplant settings, the innate immune system can distinguish between self and non-self and induce and maintain alloreactive responses [19–21] and indicate a need to determine the exact roles of GILs with a memory phenotype in the very early post-transplantation phase. Therefore, we investigated the immune function of GILs with a focus on alloreactivity.

There are some challenges in evaluating GIL functions, particularly alloreactivity. First, the number of early-phase GILs is insufficient to perform functional assays (e.g., mixed lymphocyte reactions). Second, nonspecific inflammation immediately after transplantation may affect the GIL activation status, which interferes with the identification of lymphocytes that respond to alloantigens from other activated cells. Third, because immunological reactions involve dynamic interactions between various immune cells, it might be difficult to determine their potential immunological function by performing a cross-sectional analysis of their effects. Thus, it is challenging to analyze allospecific immune functions using GILs alone.

Developments regarding immunodeficient mice that exhibit targeted Rag2 and IL-2Rγc mutations, which cause a lack of adaptive immunity [22] have allowed the engraftment of low numbers of lymphocytes while preserving their immunological function *in vivo* [23]. In this study, we established an *in vivo* analysis system to reconstitute GIL immunity by adoptive transfer into these mice. We aimed to examine the immunobiological functions of GILs during the early post-transplantation phase using this reconstitution model, then identify differences in immunological behavior.

Materials and methods

Mice

All mouse strains were bred and housed in specific pathogen-free conditions. BALB/c, C57BL/6 (B6) and C3H mice were purchased from Japan SLC (Hamamatsu, Japan). C;129S4-$Rag2^{tm1.1Flv}$ $Il2rg^{tm1.1Flv}$/J (BALB/c $Rag2^{-/-}$ $\gamma c^{-/-}$ [BRG]) mice [22] were purchased from the Jackson Laboratory (Bar Harbor, ME, USA) and maintained in Hokkaido University Institute for Animal Experimentation. All experimental procedures involving mice were performed in accordance with the Institutional Animal Care and Use Guidelines of Hokkaido University.

Murine heterotopic heart transplantation

Heart transplantation in mice was performed using a previously described method [24]. During heart graft retrieval, the donor pulmonary artery and ascending aorta were incised, remaining heart vessels were ligated, and the heart was removed. The donor ascending aorta and pulmonary artery were anastomosed to the recipient abdominal aorta and inferior vena cava, respectively. Heart graft survival was monitored daily by palpation; complete cessation of heartbeat was regarded as rejection.

Heart re-transplantation

BALB/c first recipient mice were generally anesthetized using isoflurane, then underwent repeat laparotomy; blood flow in the abdominal aorta and inferior vena cava was interrupted using a vascular clamp device. The graft was immediately flushed with heparinized saline solution until red blood cells were absent from the right ventricle. The graft was procured by cutting the graft aorta and pulmonary artery at the point of anastomosis. Allografts retrieved from first recipients were re-transplanted immediately into BRG second recipient mice by the method used during primary transplantation. A CD25-depleting antibody (PC61, 500 μg per mouse at 30 days post-retransplantation; Bio X Cell, Lebanon, NH, USA) and an anti-PD-1 blockade antibody (J43, 500 μg per mouse at day 30, 250 μg per mouse at day 32 and 34 post-retransplantation, Bio X Cell) were injected intraperitoneally.

Isolation of GILs

The cardiac graft retrieval procedure was identical to the method described above for heart re-transplantation. Retrieved heart grafts were finely cut and incubated at 37°C for 30 min in Roswell Park Memorial Institute Medium (RPMI) 1640 plus 5 mg collagenase IV (Sigma-Aldrich, St. Louis, MO, USA). Mononuclear cells were isolated by gradient centrifugation using Lympholyte M (Cedarlane Laboratories Ltd., Burlington, Canada). Total retrieved cells were counted using a hemocytometer.

Cell transfer and reconstitution

Isolated GILs were suspended in 200 µl RPMI 1640 and immediately transferred to BRG mice by intraperitoneal injection. To confirm whether mice had been reconstituted with injected cells, flow cytometric analysis of peripheral blood was performed weekly.

Flow cytometry

Spleen cells, blood cells and GILs were stained and analyzed on a FACS Canto II flow cytometer (BD Biosciences, Franklin Lakes, NJ, USA), and resulting data were processed using FlowJo version 7.6.5 software (BD Biosciences). Fluorochrome-conjugated antibodies used for flow cytometry were as follows: anti-mouse CD3ϵ (clone 145-2C11), CD4 (GK1.5), CD8a (53-6.7), CD11b (M1/70), CD11c (N418), CD25 (PC61), CD40 (3/23), CD44 (IM7), CD45 (30-F11), CD49d (R1-2), CD62L (MEL-14), CD69 (H1.2F3), CD86 (GL1), CD103 (2E7), Nur77 (12.14), T-bet (4B10), GATA3 (L50-823), RORγt (Q31-378), Foxp3 (FJK-16s), H-2Kb (AF6-88.5.5.3), H-2Kd (SF1-1.1.1), I-A/I-E (M5/114.15.2), IFNγ (XMG1.2), TNFα (MP6-XT22), Granzyme B (NGZB), and Perforin (S16009A) (antibodies were purchased from BD Biosciences, BioLegend, San Diego, CA, USA or Thermo Fisher Scientific, Waltham, MA, USA). Dead cells were excluded from all analysis by using 7-AAD staining solution (BD Biosciences). Intracellular expressions of T-bet, GATA3, RORγt, Foxp3 and Nur77 were determined using a Foxp3/Transcription Factor Staining Buffer Kit (Thermo Fisher Scientific) in accordance with the manufacturer's instructions. For intracellular cytokine staining, cells were fixed and permeabilized with Cytofix/Cytoperm solution (BD Biosciences), followed by staining with fluorochrome-labeled cytokine antibodies, in accordance with the manufacturer's instructions.

ELISpot assay

Isolated spleen cells were co-cultured with irradiated donor/third-party/autologous spleen cells in ELISpot MultiScreen Filter Plates (Millipore Corporation, Burlington, VT, USA) that had been precoated with an IFNγ capture antibody (BD Biosciences); the cells were incubated for 24h at 37°C in a 5% CO_2 atmosphere. IFNγ spots were detected using a detection antibody (BD Biosciences) and visualized using streptavidin-ALP, then incubated with a substrate solution. Spots were counted by ImmunoSpot software (Cellular Technology Limited, Shaker Heights, OH, USA).

Morphometric analysis

Procured cardiac grafts were frozen at −80°C. Frozen specimens were sectioned at a thickness of 5 µm using a cryostat (CM 1860, Leica, Wetzlar, Germany). The sections were stained with hematoxylin/eosin and imaged by light microscopy (BZ-X800, Keyence, Osaka, Japan).

Immunohistochemistry

Frozen sections (10 µm) of heart graft samples were fixed by incubation in 4% paraformaldehyde for 15 min. They were then incubated overnight at 4°C with anti-mouse CD3ϵ (EPR20752) primary antibody. Samples were subsequently incubated for 45 min at room temperature with Dako EnVision[+] System-Rabbit HRP (Agilent, Santa Clara, CA, USA), then subjected to DAB (Cell Signaling Technology, Danvers, MA, USA) staining until a brown color was visible. Positive cells were confirmed by high magnification (400×) visualization using light microscopy.

Statistical analysis

Data are shown as the mean ± SD and were analyzed with Prism version 7.0a (GraphPad Software, San Diego, CA, USA). Variables were compared using Student's t-test. Graft survival was analyzed using the Kaplan-Meier method, then compared by the log-rank test. The sample size chosen for animal experiments was estimated based on the literature and our previous experience in performing similar experiments. Differences were considered statistically significant when $P < 0.05$.

Results

Type I immune responses were significantly increased in GILs at 120 h post-transplantation

Subsets of GILs during early phase post-transplantation were assessed by flow cytometry. Total numbers of GILs were similar between syngeneic and allogeneic grafts in BALB/c recipient mice at 72 h post-transplantation; however, significantly greater numbers of GILs were obtained from allogeneic grafts at 120 h (Fig. 1a). We also esxamined the origin of GILs by measuring MHC class I expression. Notably, most CD3$^+$ cells in the graft 72 h post-transplantation were recipient-derived (Fig. 1b). Among CD3$^+$ GILs, significantly greater numbers of CD8$^+$ lymphocytes were observed in the graft at 120 h compared with the numbers of CD8$^+$ lymphocytes in the graft at 72 h (Fig. 1c). In terms of naïve/memory populations, there were no significant differences among the 72-h and 120-h GILs, including in syngeneic grafts where CD44^{hi}CD62L^{lo} effector memory T cells were the dominant population in both CD4$^+$ and CD8$^+$ GILs (Fig. 1c). Moreover, a differentiated CD4$^+$ lineage in GILs that was skewed toward T helper (Th)1 cells was predominant at 120 h post-transplantation; a significantly increased level of T-bet was observed in CD4$^+$ GILs at 120 h, compared with the level at 72 h post-transplantation (Fig. 1d, $P < 0.001$). There were no significant difference between groups in the expression levels of GATA3 and RORγt in CD4$^+$ GILs (Fig. 1d). Although the Foxp3 expression level in CD4$^+$ GILs was significantly increased in GILs at 120 h, increased percentages of CD25$^+$Foxp3$^-$CD4$^+$ GILs were also observed (Fig. 1e). Taken together, the dynamic changes in the properties of GILs at 72 h and 120 h post-transplantation suggest that distinct subsets of GILs at 120 h (e.g., Th1 cells) might be involved in alloimmune responses.

GILs in allografts were significantly activated at 120 h but not 72 h post-transplantation

Significant increases in the numbers of CD25$^+$ cells among both CD4$^+$ and CD8$^+$ GILs at 120 h (Figs 1e and 2a) indicated that 120-h GILs were in an activated state. Therefore, we examined their activation status and cytokine production ability. In addition to CD25, we observed increased expression levels of CD69, T-bet, and Nur77 among CD4$^+$ and CD8$^+$ GILs (Fig. 2a). The upregulation of T-bet in CD8$^+$ T cells reportedly indicates the acquisition of an effector phenotype [11,25]. Moreover, Nur77 is upregulated by TCR signaling in

lymphocytes [26–28]; these findings indicated the presence of stimulated T cells, achieved through TCR signaling. A significantly greater expression level of Nur77 was observed in CD69$^+$T-bet$^+$ CD4$^+$ and CD8$^+$ GILs at 120 h (Fig. 2b), suggesting that alloantigen-activated T cells exhibited a CD69$^+$T-bet$^+$ phenotype. Significant enhancements of CD69 and T-bet expression levels were observed in both CD4$^+$ and CD8$^+$GILs at 120 h (Fig 2c). Additionally, at 120 h post-transplantation, CD69$^+$T-bet$^+$ lymphocytes were observed only in the graft site (Fig. S1A). To determine whether CD8$^+$ GILs had cytotoxic properties, the levels of proinflammatory cytokines (e.g., IFNγ, TNFα, perforin, and granzyme B) were investigated. At 72 h post-transplantation, CD8$^+$ GILs produced small amounts of proinflammatory cytokines in allogeneic and syngeneic grafts (Fig. 2d). In contrast, proinflammatory cytokines were extensively produced in 120-h CD8$^+$ GILs (Fig. 2d). This increased cytokine production was observed only in the graft (Fig. S1B). Overall, GILs at 120 h but not 72 h post-transplantation were presumably activated by TCR stimulation and acquired cytotoxic activity.

Early phase GILs could be reconstituted in immunodeficient mice, and reconstituted GILs had distinct alloreactivities over time after transplantation

We showed that GILs in the allografts at 72 h post-transplantation did not have an activated phenotype. However, the ability of 72-h GILs to respond to alloantigens and cause graft rejection remained unclear. Thus, we attempted to assess the alloreactivity using BRG mice, which lack lymphocytes-mediated immunity [22], by adoptively transferring lymphocytes to reconstitute their immunity. GILs were isolated at 72 or 120 h posttransplantation and adoptively transferred into immunodeficient mice by intraperitoneal injection (Fig. 3a). The numbers of transferred GILs were 1.0–2.5×10^4 per mouse. Transferred lymphocytes were sufficiently reconstituted; the reconstitution rates of CD3$^+$ T cells in peripheral blood (Fig. 3b) were similar between the two groups. At 70 days after transfer, we obtained sufficient numbers of lymphocytes from the spleens of reconstituted BRG mice (Fig. 3c). The proportions of CD3$^+$, CD4$^+$ and CD8$^+$ T cells in the spleen were also similar between the two groups (Fig. 3d). There were no significant differences in the proportions of cells with a memory phenotype. The predominant subset in CD4$^+$ T cells had a CD44^{hi}CD62^{lo} effector memory phenotype; similar proportions of central memory (CD44^{hi}CD62L^{hi}) and effector memory phenotype were
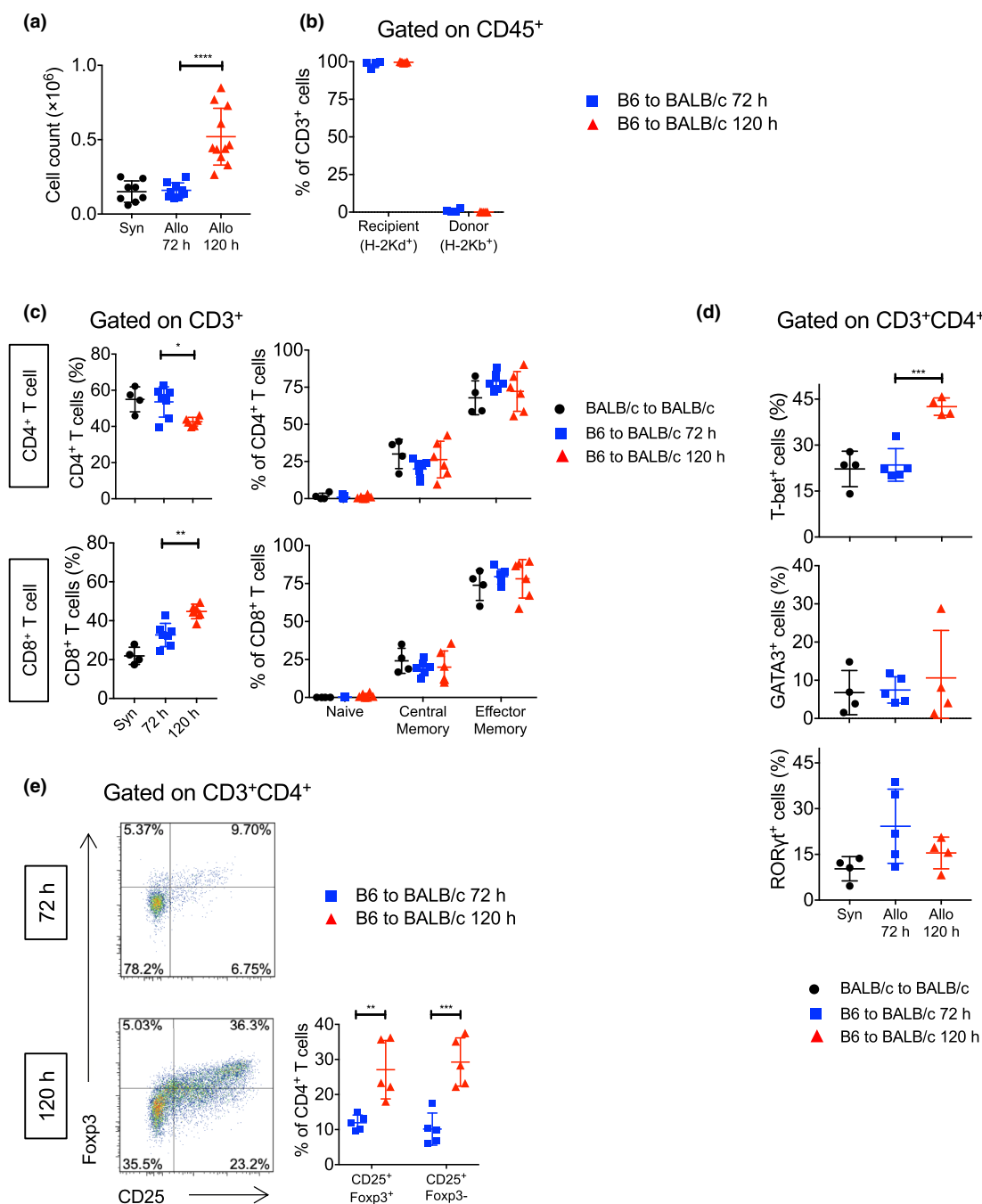
Figure 1 Population of early-phase graft-infiltrating lymphocytes of cardiac allografts. Cardiac allografts were retrieved at 72 h or 120 h post-transplantation. Retrieved allografts were finely cut into small pieces and then incubated in RPMI 1640 plus collagenase IV for 30 min. Graft-infiltrating lymphocytes (GILs) were isolated by gradient centrifugation. Subsets of GILs were assessed by flow cytometric analysis (black circles; GILs from 72-h syngeneic grafts, blue squares; GILs from 72-h allogeneic grafts, red triangles; GILs from 120-h allogeneic grafts). (a) Total numbers of GIL ($n = 8–11$ per group). (b) MHC class I expression on CD3$^+$ GILs, indicating GIL origin ($n = 4$ per group). (c) Proportions of CD4$^+$ (left upper figure) and CD8$^+$ (left lower figure) GILs. Naïve/memory population of CD4$^+$ (right upper figure) and CD8$^+$ (right lower figure) GILs. Each population was defined as naïve: CD44^{lo}CD62L^{hi}, central memory: CD44^{hi}CD62L^{hi}, and effector memory: CD44^{hi}CD62L^{lo} ($n = 4–6$ per group). (d) Expression levels of transcription factors T-bet (upper figure), GATA3 (middle figure) and RORγt (lower figure) in CD4$^+$ GILs ($n = 4–5$ per group). (e) Expression levels of CD25 and Foxp3 in CD4$^+$ GILs at 72 h or 120 h post-transplantation. Each experiment was performed at least four times independently. Statistical significance was determined by the Student's t-test for indicated pairwise comparisons. *$P < 0.05$, **$P < 0.01$, ***$P < 0.001$, ****$P < 0.0001$.
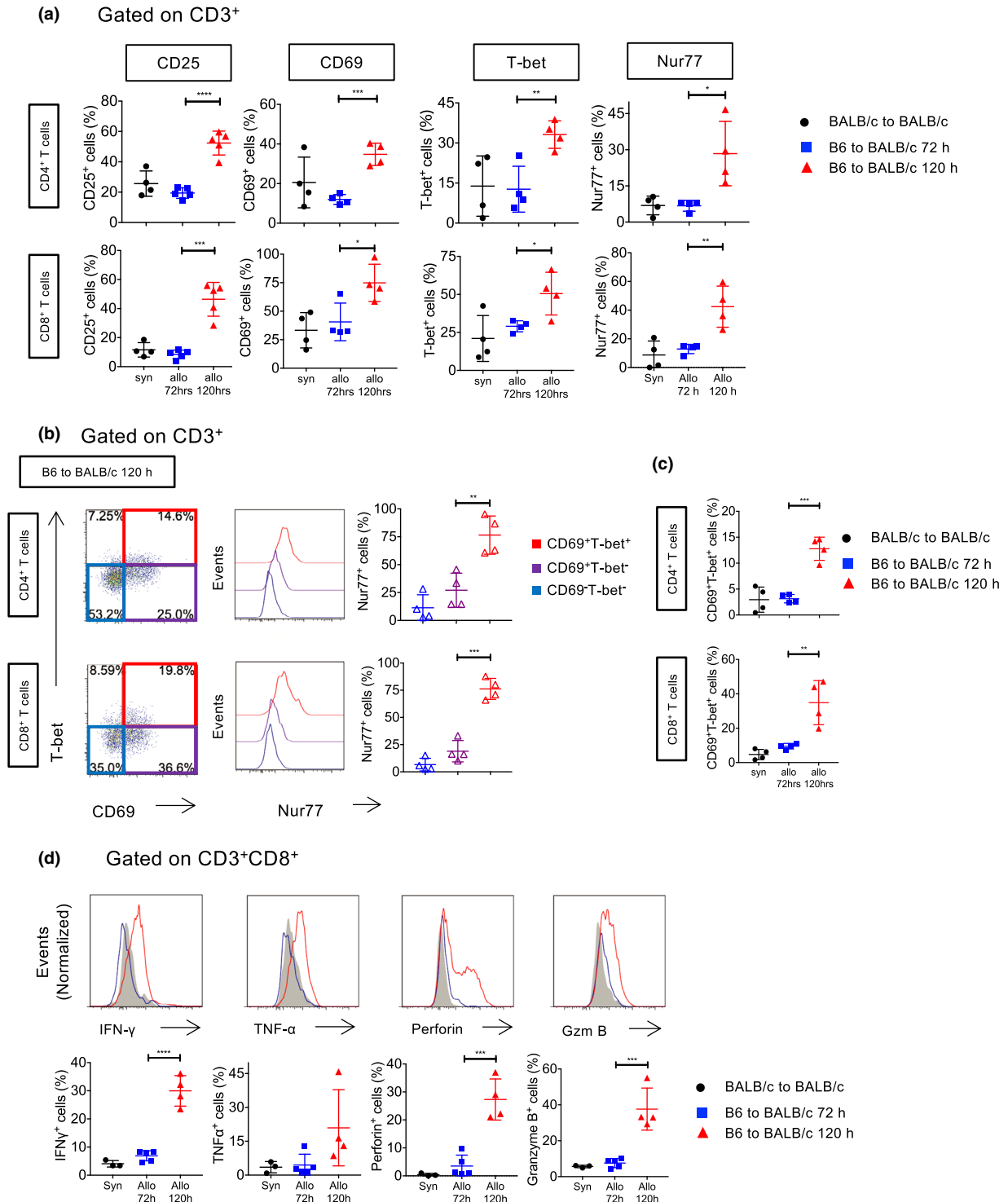
Figure 2 GILs at 120h but not 72h post-transplantation are significantly activated. Activation statuses of GILs isolated from 72-h syngeneic (black circles), 72-h allogeneic (blue squares), or 120-h allogeneic (red triangles) grafts was assessed by flow cytometric analysis. (a) Proportions of CD25$^+$, CD69$^+$, T-bet$^+$, and Nur77$^+$ cells among CD4$^+$ (upper row) and CD8$^+$ (lower row) GILs. (b) Nur77 expression levels in CD69$^+$T-bet$^+$ (red lines and triangles), CD69$^+$T-bet$^-$ (purple lines and triangles) and CD69$^-$T-bet$^-$ (blue lines and triangles) populations in CD4$^+$ (upper row) and CD8$^+$ (lower row) 120-h GILs. (c) Proportions of CD69$^+$T-bet$^+$ cells among CD4$^+$ (upper row) and CD8$^+$ (lower row) GILs. (d) Proinflammatory cytokine production by CD8$^+$ GILs from 72-h syngeneic (gray lines and circles), 72h allogeneic (blue lines and squares) or 120-h allogeneic (red lines and triangles) grafts. Each experiment was performed at least three times independently ($n = 3$–5 for each group). Statistical significance was determined by Student's *t*-test for the indicated pairwise comparisons. *$P < 0.05$, **$P < 0.01$, ***$P < 0.001$, ****$P < 0.0001$.

observed among CD8$^+$ T cells (Fig. 3e). Among CD4$^+$ T cells, the proportions of CD25$^+$Foxp3$^+$ regulatory T cells were similar between mice reconstituted with 72-h GILs and mice reconstituted with 120-h GILs (Fig. 3f).

After reconstitution, we assessed in vitro and in vivo alloreactivities. In the IFNγ-ELISpot assay, lymphocytes obtained from mice reconstituted with 120-h GILs produced significantly greater levels of IFNγ after donor antigen stimulation (Fig. 3g). In contrast, low IFNγ production against donor antigen was observed in mice reconstituted with 72-h GILs (Fig. 3g). Next, we transplanted cardiac allografts from B6 (H2-K^b) mice into mice reconstituted with GILs. In mice reconstituted with 120-h GILs, B6 allografts were rapidly rejected (MST = 6 days, Fig. 3h) whereas B6 allografts survived indefinitely in mice reconstituted with 72-h GILs (MST > 100 days, Video S1). Histopathological analyses of rejected allografts in mice reconstituted with 120-h GILs showed tissue destruction, morphologic features of injured cardiomyocytes (HE finding, upper left image in Fig. 3i), and extensive infiltration of CD3$^+$ T lymphocytes (immunohistochemistry, upper right image in Fig. 3i). In contrast, the histopathological features of long-term surviving grafts (100 days) in mice reconstituted with 72-h GILs showed well-preserved cardiomyocyte structures (HE, lower left in Fig. 3i), although CD3$^+$ T cells infiltration was observed (immunohistochemistry, lower right in Fig. 3i). Comparable lymphocyte subsets (Fig. S2A,B) and alloreactivities in the IFNγ-ELISpot assay (Fig. S2C) were evident in the spleens of mice reconstituted with 72-h GILs, both before and after transplantation. These findings indicated that heart transplantation did not affect reconstituted T-cell immunity in mice reconstituted with 72-h GILs. Overall, 72-h GILs had weak responsiveness to donor antigens, whereas 120-h GILs exerted potent donor antigen-specific reactivity.

Phenotypic differences in GILs were observed between 72 and 120 h post-transplantation

Because the adoptive transfer model showed distinct donor reactivities between 72-h and 120-h GILs, we investigated whether donor-reactive lymphocytes in 120-h GILs were derived from 72-h GILs or newly infiltrated lymphocytes that arrived after 72 h. When we examined the activation statuses of host DCs in grafts, we found that expression levels of CD86 and CD40 were higher at 120 h post-transplantation than at 72 h post-transplantation (Fig. 4a). Additionally, the proportion of host CD103$^+$ DCs in the graft (i.e., cells

presumed to activate antigen-specific lymphocytes [29]), tended to be higher at 120 h than at 72 h ($P = 0.09$, Fig. 4b). These data implied that APCs in the graft could influence the GILs' activation status. To investigate the origin of alloreactive T cells observed in 120-h GILs, we attempted to prevent newly infiltrating lymphocytes from entering the graft at 72–120 h post-transplantation by integrin blockade using an anti-LFA antibody [8] or by the removal of secondary lymphoid tissues via splenectomy [30] at 72 h. We then assessed the donor reactivities of 120-h GILs by adoptive transfer experiments (Fig. 5a,b). The reconstitution rates were comparable between mice that received adoptive transfer of anti-LFA antibody-treated 120-h GILs and mice that underwent splenectomy (Fig. 5c–e). However, potent donor-antigen reactivities were also observed by IFNγ-ELISpot assays (Fig. 5f). Accordingly, anti-LFA antibody experiments and the removal of secondary lymphoid tissue did not prevent the development of effector T cells with potent donor reactivities in grafts at 120 h post-transplantation.

Seventy-two-hour GILs did not show alloreactivity during continuous exposure to alloantigen

In the above experiments involving splenectomy and separate adoptive transfer procedures with an anti-LFA antibody, 72-h GILs exhibited potential alloreactivity and could be terminally differentiated into locally-activated lymphocytes at 72–120 h in the graft site. However, because activated lymphocytes can use other integrins (e.g., VLA-4) to infiltrate into peripheral tissue [31,32] and be matured at the other secondary lymphoid tissues (e.g., mediastinal lymph nodes) [33], complete inhibition of infiltration might have failed and the alloreactivity may have been caused by newly infiltrated GILs. Therefore, we attempted to transfer a whole 72-h heart graft that harbored GILs, host DCs, and microenvironment (e.g., donor antigens) into BRG mice by re-transplantation; this approach could also completely remove newly infiltrating lymphocytes from 72-h post-transplantation (Fig. 6a). Importantly, re-transplanted B6 cardiac grafts continued to function for more than 100 days after re-transplantation (Fig. 6b, Video S2). Histopathological analyses of long-term re-transplanted grafts demonstrated well-preserved cardiomyocyte structures (left image in Fig. 6c). CD3$^+$ GILs were also observed in the allograft (right image in Fig. 6c), suggesting that CD3$^+$ GILs were exposed to alloantigen but did not induce allograft rejection. In these re-transplant experiments, GILs were also reconstituted in BRG mice
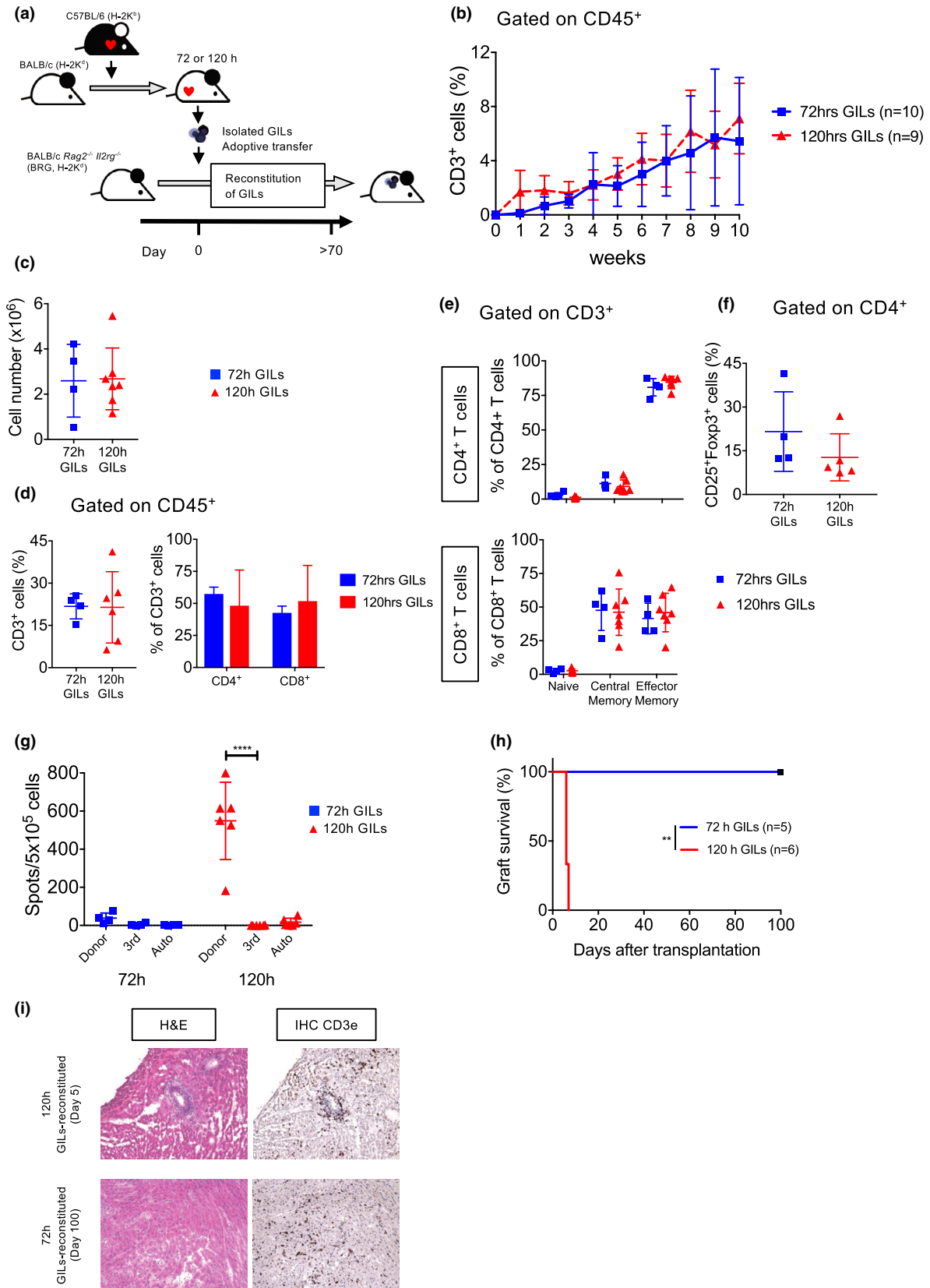
Figure 3 The BRG mice displayed donor-specific alloreactivity *ex vivo* and *in vivo* when reconstituted with 120-h but not 72-h GILs. GILs obtained from cardiac allografts at 72 or 120 h post-transplantation were adoptively transferred into BRG mice via intraperitoneal injection. The numbers of transferred cells were as follows; 72 h: $1.0–2.5 \times 10^5$; 120 h, $1.0–2.0 \times 10^5$. (a) Scheme of adoptive transfer of GILs in the early post-transplantation phase. (b) Reconstitution rates of $CD3^+$ lymphocytes in peripheral blood of BRG mice reconstituted with 72-h (blue squares, $n = 10$) and 120-h (red triangles, $n = 9$) GILs. (c–f) Lymphocyte subsets of spleens obtained from BRG mice reconstituted with 72-h GILs (blue squares, n = 4) and 120-h GILs (red triangles, $n = 5–6$) at 70 days after adoptive transfer. (c) Absolute numbers of lymphocytes in the spleen. (d) Proportions of $CD3^+$ (left figure), $CD4^+$ and $CD8^+$ (right figure) T cells. (e) Naïve $CD44^{lo}CD62L^{hi}$, central memory $CD44^{hi}CD62L^{hi}$, and effector memory $CD44^{hi}CD62L^{lo}$ populations of $CD4^+$ (upper row) and $CD8^+$ (lower row) T cells. (f) Proportions of $CD25^+Foxp3^+$ Tregs among $CD4^+$ T cells. (g) Lymphocytes (5×10^5) isolated from spleens of BRG mice reconstituted with 72-h GILs (blue squares, $n = 4$) and 120-h GILs (red triangles, $n = 6$) at 70 days after adoptive transfer were co-cultured with 5×10^5 irradiated spleen cells obtained from donor or third-party (C3H) strains of mice. Frequencies of IFNγ-producing cells were assessed using ELISpot. (h–i) Donor strain B6 cardiac allografts were transplanted into BRG mice reconstituted with 72-h GILs (blue line, $n = 5$), 120-h GILs (red line, $n = 6$). (h) Graft survival rate in BRG mice. (i) Representative images of H&E histological staining (left column) and immunohistochemical staining with anti-mouse CD3ε antibody (right column) results using cardiac allografts obtained from BRG mice reconstituted with 120-h GILs at 5 days post-transplantation (upper row) and BRG mice reconstituted with 72-h GILs at 100 days post-transplantation (lower row). Each experiment was performed twice independently. Statistical significance was determined by Student's *t*-test for the indicated pairwise comparisons, Log-rank test for graft survival and two-way ANOVA for ELISpot assays. **$P < 0.01$, ****$P < 0.0001$.

that contained populations similar to the isolated GILs used in adoptive transfer experiments (Figs 3d,e and 6d, e). Then, alloreactivities were evaluated in lymphocytes obtained from spleens of BRG mice that had been re-transplanted with 72-h grafts by IFNγ-ELISpot assay at 100 days after re-transplantation, and low IFNγ production levels against donor and third-party antigens were observed (Fig. 6f). When anti-CD25 antibody treatment was administered at 30 days after retransplantation to deplete $CD4^+CD25^+$ Tregs, no graft rejection was observed immediately after the depletion of $CD4^+$Tregs (Fig. S3A). Additionally, when anti-PD-1 blocking antibodies were administered at 30, 32 and 34 days after retransplantation, graft rejection did not occur (Fig.

S3A). The histopathological findings (Fig. S3B) and the reconstitution rates (Fig. S3C,D) were comparable between mice that received anti-CD25 and anti-PD-1 treatment. These findings indicated that $CD4^+CD25^+$ Tregs and T cell-exhaustion were not critical for allograft preservation in the presence of reconstituted lymphocytes. Overall, GILs at 72 h post-transplantation failed to exhibit donor-antigen reactivity, despite their presence in allografts in re-transplantatiom models while they secreted low levels of proinflammatory cytokines in an alloantigen-nonspecific manner. Furthermore, $CD4^+CD25^+$ Tregs and exhaustion were not critical for allograft preservation in the presence of reconstituted lymphocytes. GILs at 72 h did not have
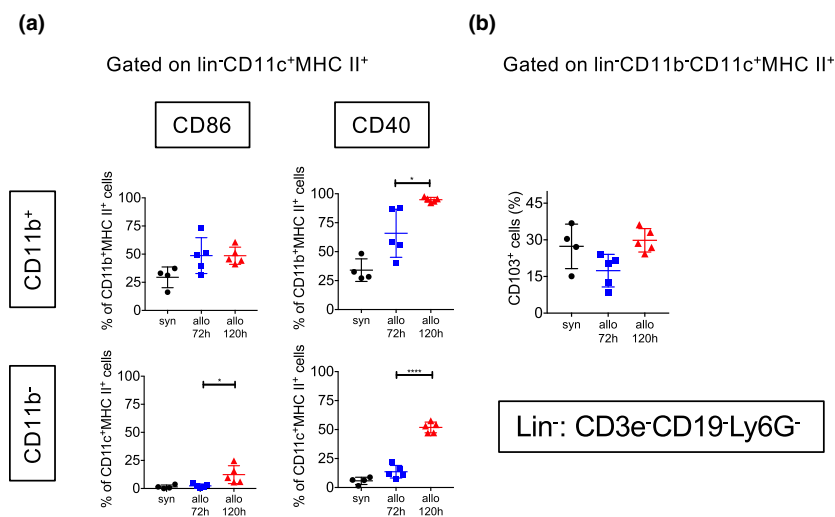

Figure 4 Activation status of graft site APCs. (a-b) Graft-infiltrating mononuclear cells were isolated from recipients at 72 h or 120 h and the activation status and population of T cell-activating DCs were analyzed by flow cytometry. DCs: Lineage$^-$CD11c$^+$MHC class II$^+$. (a) APC activation marker expression. Percentages of $CD86^+$ and $CD40^+$ cells among $CD11b^+$ (upper row) and $CD11b^-$ (lower row) DCs. (b) Percentages of $CD103^+$ cells among $CD11b^-CD11c^+MHC II^+$ DCs. These experiments were performed three times independently. Statistical significance was determined by Students *t*-test for the indicated pairwise comparisons. *$P < 0.05$, ****$P < 0.0001$.

alloantigen-specific cytotoxicity, although they secreted low levels of proinflammatory cytokines in an alloantigen-nonspecific manner.

Discussion

In organ transplantation, T lymphocytes are an important source of immune reactions against allografts; notably, alloantigen-specific T cells can induce acute rejection. Therefore, it is important to determine the source of alloantigen-specific T cell-mediated immune reactions. In this study, lymphocytes with a memory phenotype in allogeneic grafts at 72 h, which had a weak response to alloantigens, did not reject the allograft *in vivo*; conversely, 120-h GILs responded to an alloantigen and directly rejected heart allografts *in vivo* (Fig. 3g,h).
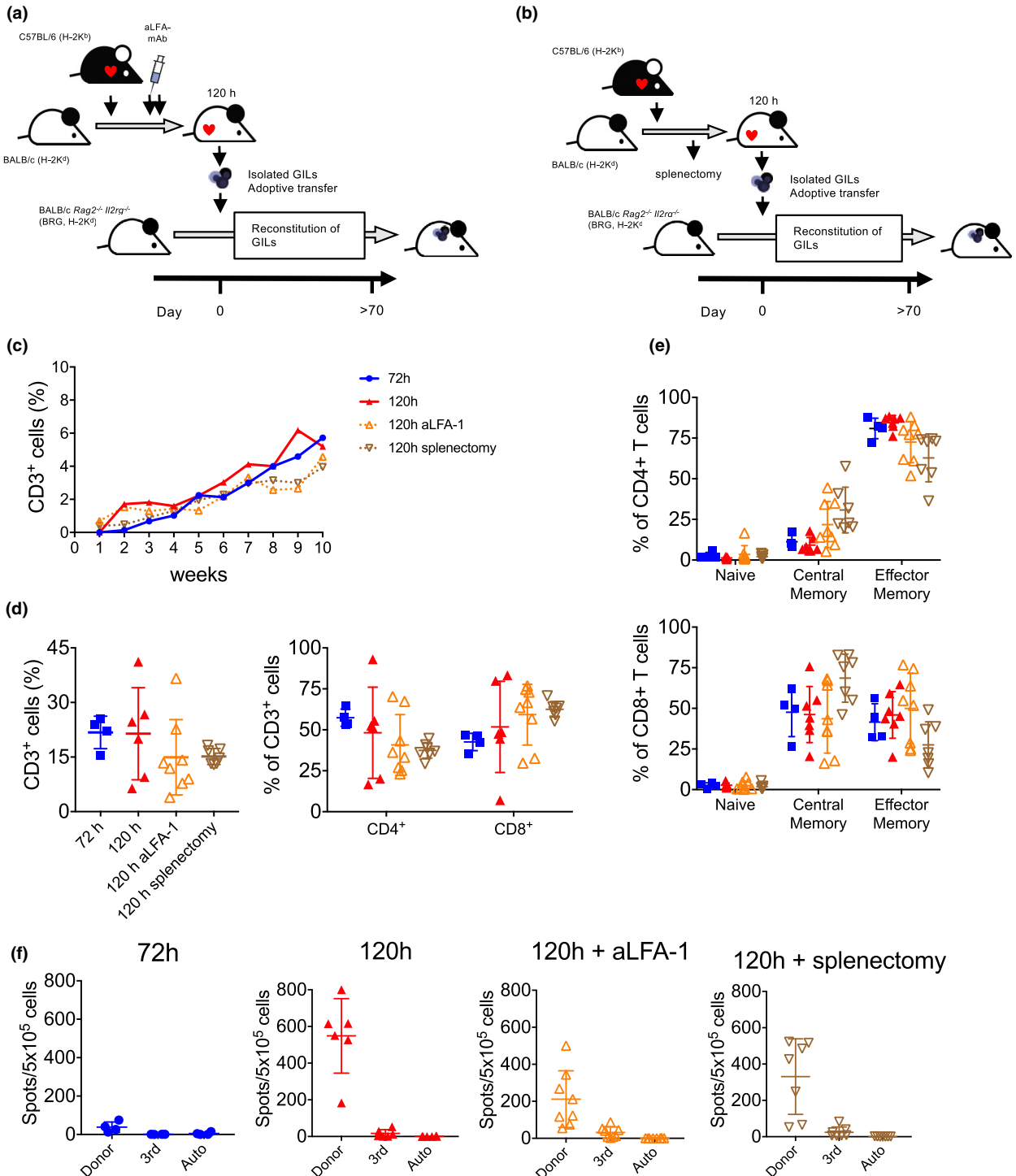
Figure 5 Functional analysis of GILs at 120 h with anti-LFA-1 mAbs treatment at 72 h and 96 h or splenectomy at 72 h. C57BL/6 heart allografts were transplanted into BALB/c recipients. At 72 h post-transplantation, anti-LFA mAbs are injected intraperitoneally or splenectomy was performed in the recipient. GILs isolated from allografts procured at 120 h were adoptively transferred into BRG mice intraperitoneally. The numbers of transferred cells were as follows: 72 h: $1.0–2.5 \times 10^5$, 120 h: $1.0–2.0 \times 10^5$, 120 h + aLFA-1: $1.0–2.5 \times 10^5$, and 120 h + splenectomy: $1.0–2.5 \times 10^5$. (a) Scheme of the adoptive transfer of GILs with anti-LFA mAb treatment. (b) Scheme of the adoptive transfer of GILs with splenectomy. (c) The reconstitution rates of $CD3^+$ lymphocytes in peripheral blood in the 72 h (blue), 120 h (red), 120 h + anti-LFA-1 (orange), and 120 h + splenectomy (brown) groups. (d) The proportion of reconstituted $CD3^+$ cells among $CD45^+$ cells (left figure) and the proportion of $CD4^+$ and $CD8^+$ T cells among $CD3^+$ cells (right figure) in the spleen. (e) Naïve, $CD44^{lo}CD62L^{hi}$, central memory, $CD44^{hi}CD62L^{hi}$, and effector memory, $CD44^{hi}CD62L^{lo}$, populations of $CD4^+$ (upper figure) and $CD8^+$ (lower figure) T cells. (f) Lymphocytes (5×10^5) isolated from spleens of BRG mice reconstituted with 72-h GILs (left figure, blue squares, $n = 4$), 120-h GILs (center figure, red filled triangles, $n = 6$), 120h + anti-LFA-1 (center figure, orange open triages, $n = 8$), or 120h + splenectomy (right figure, brown open triangles, $n = 7$) at 70 days after adoptive transfer, were co-cultured with 5×10^5 irradiated spleen cells obtained from donor (C57BL/6), 3rd party (C3H), or auto (BALB/c) strains of mice. The frequencies of IFNγ-producing cells were assessed using ELISpot. These experiments were performed twice independently. Statistical significance was determined using Student's t-test for the indicated pairwise comparisons, Log-rank test for graft survival, and two-way ANOVA for ELISpot assays.

Our results indicated that early-phase GILs changed their phenotype over time after transplantation.

Biomarkers for T-cell activation have been developed. The expression level of T-bet is associated with distinct stages of T-cell activation and function [11]. We demonstrated that activated T cells expressing CD69 had high and low levels of T-bet (Fig. 2b) suggesting that 120-h GILs may include short-lived and precursor memory effector T cells [25]. Nur77 is a biomarker upregulated by TCR stimulation, but not cytokine activation [28]. Significantly elevated expression levels of Nur77 in $CD69^+T-bet^+$ cells among $CD4^+$ and $CD8^+$ GILs at 120 h post-transplantation (Fig. 2b) suggest that T-bet and Nur77 may serve as candidate biomarkers for alloreactive T cells in a transplant setting.

To directly assess the exact roles and functions of a small population of GILs, we reconstituted lymphocytes in immunodeficient mice. Although we demonstrated clear differences in immunological behavior between 72-h and 120-h GILs in our model, there were some important considerations. First, during reconstitution, proliferated lymphocytes expressed CD44, regardless of antigen exposure (i.e., homeostatic expansion); this indicated the conversion of naïve lymphocytes into a memory population (i.e., virtual memory or memory phenotype lymphocytes) [13,14,34,35] which could influence their immune behavior. We found a significant increase in the virtual memory phenotype ($CD49d^-CD44^+$ T cells, regarded as an antigen-inexperienced phenotype) among $CD8^+$ T cells in reconstituted lymphocytes from 72-h GILs, compared with 120-h GILs (Fig. S4). This suggests that T cells with an antigen-inexperienced memory phenotype might be generated during homeostatic proliferation in mice reconstituted with 72-h GILs. While lymphocytes with a $CD49d^-$ phenotype are presumed to produce

proinflammatory cytokines by an antigen-specific mechanism [34,35] it remains unclear whether these subsets exert strong responses that cause alloantigen rejection. Second, ongoing lymphocyte proliferation could modulate resistance against transplant tolerance [36–38]. Because lymphocytes might be immunologically distorted during ongoing homeostatic proliferation [36,37], we assessed lymphocytes when homeostatic proliferation was presumably completed. Although the effects of homeostatic proliferation cannot be ignored in an adoptive transfer model, we identified the functional differences among isolated cell lineages *in vivo*.

Reports from Lakkis *et al.* indicated that T-cell priming and maturation in secondary lymph nodes were insufficient to induce allograft rejection; interactions between graft-infiltrating host APCs were required to maintain effector T cell reactivity [39,40]. These findings suggest the potential for ≤72-h GILs to become activated and differentiate into terminal effector T cells at the graft site. We observed that host DCs in 120-h grafts expressed significantly greater levels of activation markers, compared with host DCs in 72-h grafts (Fig. 4), which suggested interactions between alloantigen-reactive GILs and graft-infiltrating DCs. The presence of donor reactivity, despite the interruption of lymphocyte infiltration into the graft from 72 to 120 h post-transplantation through integrin blockade with anti-LFA antibodies (Fig. 5a)[8] or through the removal of secondary lymphoid tissues by splenectomy (Fig. 5b)[30] also implies that immature allospecific GILs at 72 h had subsequently matured at the graft site. However, 72-h grafts re-transplanted into immunodeficient mice, a model in which new infiltration of recipient lymphocytes is completely interrupted, were well-preserved in the absence of graft rejection; this findings suggested that lymphocytes in 72-h grafts do not gain the capability for allograft rejection. Furthermore,
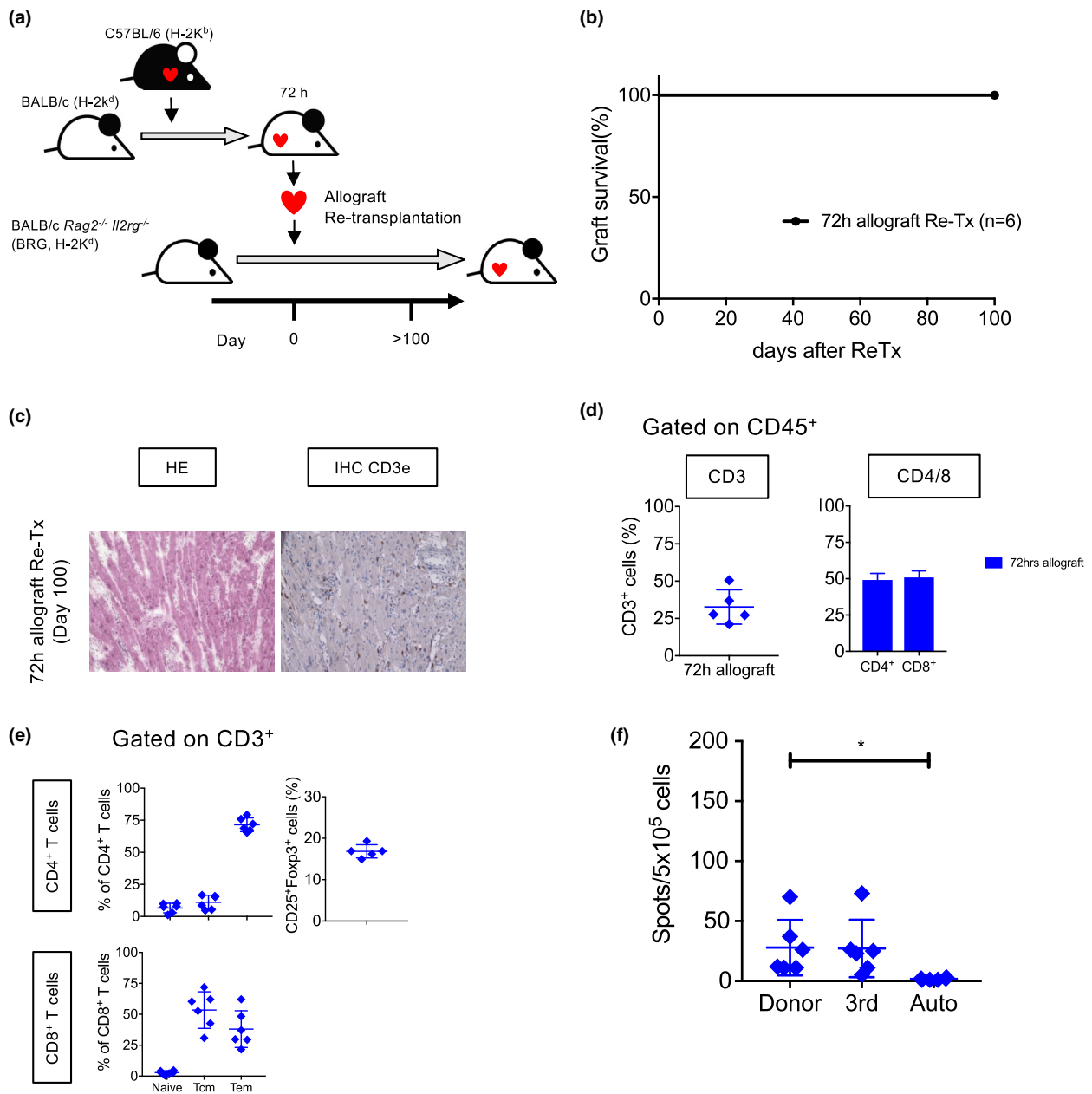
Figure 6 Cardiac allografts at 72h post-transplantation exhibit long-term function after re-transplantation in BRG mice. B6 cardiac allografts transplanted in BALB/c mice were retrieved at 72 h post-transplantation and directly re-transplanted into BRG mice. (a) Scheme of re-transplantation into BRG mice shows transplanted allografts obtained 72 h post-transplantation (B6 to BALB/c) were re-transplanted into BRG mice. (b) Re-transplanted graft survival rates in BRG mice, ReTx only ($n = 6$). (c) Representative images of H&E histological staining (left image) and immunohistochemical staining with CD3ε antibody (right image) in long-term (100 days) re-transplanted cardiac allografts of BRG mice. (d) Reconstituted populations of CD3$^+$ (left figure), CD4$^+$ and CD8$^+$ (right figure) cells in the spleens of BRG mice at 100 days post-retransplantation. (e) Populations of naïve, central memory, and effector memory (left figures) cells among CD4$^+$ (upper row), CD8$^+$ (lower row) and CD4$^+$CD25$^+$Foxp3$^+$ (right figure) cells in the spleens of BRG mice at 100 days post-retransplantation. (f) Spleen cells (5×10^5) retrieved from BRG mice at 100 days post-retransplantation were co-cultured with 5×10^5 irradiated donor or third-party (C3H) spleen cells. IFNγ alloreactivities were evaluated using ELISpot. Each experiment was performed twice independently. Statistical significance was determined by two-way ANOVA for ELISpot assays.

lymphocytes in the re-transplanted allografts were not suppressed by Treg nor exhausted against alloantigens; our findings suggest that these lymphocytes did not possess intrinsic alloantigen-specific reactivity. These

discrepancies with previous studies may be related to the incomplete elimination of newly infiltrating lymphocytes by anti-LFA antibodies [31,41] or the presence of other effector lymphocytes that were primed outside the spleen

(e.g., mediastinal lymph nodes) [33]; donor-reactive lymphocytes might infiltrate into the graft from 72 to 120 h and display donor reactivity in reconstituted mice (Fig. 5f). To confirm this hypothesis, further investigations are warranted.

There is an urgent need to elucidate the precise immune behavior of early phase GILs with a memory phenotype, particularly for determination of the appropriate time to initiate immunosuppression after transplantation when aiming to achieve long-term preservation of a well-functioning graft. At the early stage of inflammation, lymphocytes with a memory phenotype rapidly infiltrate into pathogenic sites [42], respond to proinflammatory cytokines[43], differentiate into IFNγ-secreting lymphocytes [44], and promote further recruitment and activation of multiple immune effector cells [44,45]. However, inhibition of the early infiltration of memory T lymphocytes reportedly abrogates the induction of transplant tolerance in mice [16–18,46]. A clinical study showed that delayed initiation of immunosuppressants at 72 h post-transplantation led to a lower incidence of acute rejection and lower doses of immunosuppressants [47,48]. These observations suggested that some early-phase GILs have immunomodulatory functions. Additionally, the immune functions of antigen-nonspecific T cells within local inflammatory lesions have been reported [49]. These cells can be activated independently of TCR signaling in localized inflammatory environments; they can be either destructive [50] or protective [51]. A precise understanding of the immunobiological behavior of alloantigen-nonspecific GILs during the early post-transplantation phase might elucidate the mechanism involved in inducing transplant tolerance and provide an approach for long-term preservation of a well-functioning graft.

In conclusion, we have identified the functional roles of GILs in the early post-transplantation phase using an adoptive transfer model in immunodeficient mice. In this model, time-dependent differences in GIL phenotype and alloreactivity were clarified in the early post-transplantation phase. A better understanding of cellular function in a graft site microenvironment *in vivo* may provide clues regarding new treatment strategies for organ transplantation.

Authorship

Funding

Conflict of interest

Acknowledgements

SUPPORTING INFORMATION

Additional supporting information may be found online in the Supporting Information section at the end of the article.

Figure S1 Alloantigen specific stimulation during early phase post-transplantation might be observed only within the graft at 120 h post-transplantation.

Figure S2 Similar lymphocyte subsets and alloreactivity before and after C57BL/6 cardiac transplantation into 72 h GILs-reconstituted BRG mice.

Figure S3 Cardiac allografts at 72h post-transplantation exhibit long-term function after re-transplantation in BRG mice.

Figure S4 CD49d expression levels of CD8+ GILs before and after reconstitution in GILs adoptive transfer models.

Video S1 Allografts transplanted into 72-h GILs-reconstituted BRG mice at 100 days after transplantation.

Video S2 Re-transplanted B6 allografts into BRG second recipient at 100 days after re-transplantation.

REFERENCES

1. Zhang N, Schroppel B, Lal G, *et al.* Regulatory T cells sequentially migrate from inflamed tissues to draining lymph nodes to suppress the alloimmune response. *Immunity* 2009; **30**: 458.

2. Kendal AR, Chen Y, Regateiro FS, *et al.* Sustained suppression by Foxp3+ regulatory T cells is vital for infectious transplantation tolerance. *J Exp Med* 2011; **208**: 2043.

3. Wood KJ, Goto R. Mechanisms of rejection: current perspectives. *Transplantation* 2012; **93**: 1.

4. Schenk AD, Nozaki T, Rabant M, Valujskikh A, Fairchild RL. Donor-reactive CD8 memory T cells infiltrate cardiac allografts within 24-h post-transplant in naive recipients. *Am J Transplant* 2008; **8**: 1652.

5. El-Sawy T, Miura M, Fairchild R. Early T cell response to allografts occuring prior to alloantigen priming up-regulates innate-mediated inflammation and graft necrosis. *Am J Pathol* 2004; **165**: 147.

6. Schenk AD, Gorbacheva V, Rabant M, Fairchild RL, Valujskikh A. Effector functions of donor-reactive CD8 memory T cells are dependent on ICOS induced during division in cardiac grafts. *Am J Transplant* 2009; **9**: 64.

7. Su CA, Iida S, Abe T, Fairchild RL. Endogenous memory CD8 T cells directly mediate cardiac allograft rejection. *Am J Transplant* 2014; **14**: 568.

8. Setoguchi K, Schenk AD, Ishii D, *et al.* LFA-1 antagonism inhibits early infiltration of endogenous memory CD8 T cells into cardiac allografts and donor-reactive T cell priming. *Am J Transplant* 2011; **11**: 923.

9. Ishii D, Schenk AD, Baba S, Fairchild RL. Role of TNFalpha in early chemokine production and leukocyte infiltration into heart allografts. *Am J Transplant* 2010; **10**: 59.

10. Setoguchi K, Hattori Y, Iida S, Baldwin WM 3rd, Fairchild RL. Endogenous memory CD8 T cells are activated within cardiac allografts without mediating rejection. *Am J Transplant* 2013; **13**: 2293.

11. Pritchard GH, Kedl RM, Hunter CA. The evolving role of T-bet in resistance to infection. *Nat Rev Immunol* 2019; **19**: 398.

12. Younes SA, Punkosdy G, Caucheteux S, Chen T, Grossman Z, Paul WE. Memory phenotype CD4 T cells undergoing rapid, nonburst-like, cytokine-driven proliferation can be distinguished from antigen-experienced memory cells. *PLoS Biol* 2011; **9**: e1001171.

13. Kawabe T, Jankovic D, Kawabe S, *et al.* Memory-phenotype CD4(+) T cells spontaneously generated under steady-state conditions exert innate TH1-like effector function. *Sci Immunol* 2017; **2**: eaam9304.

14. Kawabe T, Yi J, Kawajiri A, *et al.* Requirements for the differentiation of innate T-bet(high) memory-phenotype CD4(+) T lymphocytes under steady state. *Nat Commun* 2020; **11**: 3366.

15. Oberbarnscheidt MH, Walch JM, Li Q, *et al.* Memory T cells migrate to and reject vascularized cardiac allografts independent of the chemokine receptor CXCR3. *Transplantation* 2011; **91**: 827.

16. Liu X, Mishra P, Yu S, *et al.* Tolerance induction towards cardiac allografts under costimulation blockade is impaired in CCR7-deficient animals but can be restored by adoptive transfer of syngeneic plasmacytoid dendritic cells. *Eur J Immunol* 2011; **41**: 611.

17. Goto R, You S, Zaitsu M, Chatenoud L, Wood KJ. Delayed anti-CD3 therapy results in depletion of alloreactive T cells and the dominance of Foxp3+ CD4+ graft infiltrating cells. *Am J Transplant* 2013; **13**: 1655.

18. Krupnick AS, Lin X, Li W, *et al.* Central memory CD8+ T lymphocytes mediate lung allograft acceptance. *J Clin Invest* 2014; **124**: 1130.

19. Oberbarnscheidt MH, Zeng Q, Li Q, *et al.* Non-self recognition by monocytes initiates allograft rejection. *J Clin Invest* 2014; **124**: 3579.

20. Dai H, Friday AJ, Abou-Daya KI, *et al.* Donor SIRPalpha polymorphism modulates the innate immune response to allogeneic grafts. *Sci Immunol* 2017; **2**: eaam6202.

21. Dai H, Lan P, Zhao D, *et al.* PIRs mediate innate myeloid cell memory to nonself MHC molecules. *Science* 2020; **368**: 1122.

22. Song J, Willinger T, Rongvaux A, *et al.* A mouse model for the human pathogen *Salmonella typhi. Cell Host Microbe* 2010; **8**: 369.

23. Shultz LD, Brehm MA, Garcia-Martinez JV, Greiner DL. Humanized mice for immune system investigation: progress, promise and challenges. *Nat Rev Immunol* 2012; **12**: 786.

24. Wu J, Zhang H, Shi X, *et al.* Ablation of transcription factor IRF4 promotes transplant acceptance by driving allogenic CD4(+) T cell dysfunction. *Immunity* 2017; **47**: 1114.

25. Kallies A, Good-Jacobson KL. Transcription factor T-bet orchestrates lineage development and function in the immune system. *Trends Immunol* 2017; **38**: 287.

26. Moran AE, Holzapfel KL, Xing Y, *et al.* T cell receptor signal strength in Treg and iNKT cell development demonstrated by a novel fluorescent reporter mouse. *J Exp Med* 2011; **208**: 1279.

27. Au-Yeung BB, Zikherman J, Mueller JL, *et al.* A sharp T-cell antigen receptor signaling threshold for T-cell proliferation. *Proc Natl Acad Sci U S A* 2014; **111**: E3679.

28. Ashouri JF, Weiss A. Endogenous Nur77 Is a specific indicator of antigen receptor signaling in human T and B cells. *J Immunol* 2017; **198**: 657.

29. Kuhn NF, Lopez AV, Li X, Cai W, Daniyan AF, Brentjens RJ. CD103(+) cDC1 and endogenous CD8(+) T cells are necessary for improved CD40L-overexpressing CAR T cell antitumor function. *Nat Commun* 2020; **11**: 6171.

30. Lakkis FGA, Konieczny A, Inoue BT, Inoue Y. Immunologic 'ignorance' of vascularized organ transplants in the absence of secondary lymphoid tissue. *Nat Med* 2000; **6**: 686.

31. Iida S, Miyairi S, Su CA, *et al.* Peri-transplant VLA-4 blockade inhibits endogenous memory CD8 T cell infiltration into high-risk cardiac allografts and CTLA-4Ig resistant rejection. *Am J Transplant* 2019; **19**: 998.

32. Lin C, Zhang Y, Zhang K, *et al.* Fever promotes t lymphocyte trafficking via a thermal sensory pathway involving heat shock protein 90 and alpha4 integrins. *Immunity* 2019; **50**: 137.

33. Brown K, Badar A, Sunassee K, *et al.* SPECT/CT lymphoscintigraphy of heterotopic cardiac grafts reveals novel sites of lymphatic drainage and T cell priming. *Am J Transplant* 2011; **11**: 225.

34. Haluszczak C, Akue AD, Hamilton SE, *et al.* The antigen-specific CD8+ T cell repertoire in unimmunized mice includes memory phenotype cells bearing markers of homeostatic expansion. *J Exp Med* 2009; **206**: 435.

35. White JT, Cross EW, Burchill MA, *et al.* Virtual memory T cells develop and mediate bystander protective immunity in an IL-15-dependent manner. *Nat Commun* 2016; **7**: 11291.

36. Wu Z, Bensinger SJ, Zhang J, *et al.* Homeostatic proliferation is a barrier to transplantation tolerance. *Nat Med* 2004; **10**: 87.

37. Moxham VF, Karegli J, Phillips RE, *et al.* Homeostatic proliferation of lymphocytes results in augmented memory-like function and accelerated allograft rejection. *J Immunol* 2008; **180**: 3910.

38. Schietinger A, Delrow JJ, Basom RS, Blattman JN, Greenberg PD. Rescued tolerant CD8 T cells are preprogrammed to reestablish the tolerant state. *Science* 2012; **335**: 723.

39. Zhuang Q, Liu Q, Divito SJ, *et al.* Graft-infiltrating host dendritic cells play a key role in organ transplant rejection. *Nat Commun* 2016; **7**: 12623.

40. Hughes AD, Zhao D, Dai H, *et al.* Cross-dressed dendritic cells sustain effector T cell responses in islet and kidney allografts. *J Clin Invest* 2020; **130**: 287.

41. Walch JM, Zeng Q, Li Q, *et al.* Cognate antigen directs CD8+ T cell migration to vascularized transplants. *J Clin Invest* 2013; **123**: 2663.

42. Kohlmeier JE, Cookenham T, Roberts AD, Miller SC, Woodland DL. Type I interferons regulate cytolytic activity of memory CD8(+) T cells in the lung airways during respiratory virus challenge. *Immunity* 2010; **33**: 96.

43. Soudja SM, Ruiz AL, Marie JC, Lauvau G. Inflammatory monocytes activate memory CD8(+) T and innate NK lymphocytes independent of cognate antigen during microbial pathogen invasion. *Immunity* 2012; **37**: 549.

44. Berg RE, Crossley E, Murray S, Forman J. Memory CD8+ T cells provide innate immune protection against Listeria monocytogenes in the absence of cognate antigen. *J Exp Med* 2003; **198**: 1583.

45. Soudja SM, Chandrabos C, Yakob E, Veenstra M, Palliser D, Lauvau G. Memory-T-cell-derived interferon-gamma instructs potent innate cell activation for protective immunity. *Immunity* 2014; **40**: 974.

46. You S, Zuber J, Kuhn C, *et al.* Induction of allograft tolerance by monoclonal CD3 antibodies: a matter of timing. *Am J Transplant* 2012; **12**: 2909.

47. Dresske B, Zavazava N, Jenisch S, *et al.* WOFIE synergizes with calcineurin-inhibitor treatment and early steroid withdrawal in kidney transplantation. *Transplantation* 2003; **75**: 1286.

48. Dresske B, Haendschke F, Lenz P, *et al.* WOFIE stimulates regulatory T cells: a 2-year follow-up of renal transplant recipients. *Transplantation* 2006; **81**: 1549.

49. Lauvau G, Boutet M, Williams TM, Chin SS, Chorro L. Memory CD8(+) T cells: innate-like sensors and orchestrators of protection. *Trends Immunol* 2016; **37**: 375.

50. Kim J, Chang DY, Lee HW, *et al.* Innate-like cytotoxic function of bystander-activated CD8(+) T cells is associated with liver injury in acute hepatitis A. *Immunity* 2018; **48**: 161.

51. Christoffersson G, Chodaczek G, Ratliff SS, Coppieters K, von Herrath MG. Suppression of diabetes by accumulation of non-islet-specific CD8(+) effector T cells in pancreatic islets. *Sci Immunol* 2018; **3**: eaam6533.